Thesis for the Degree of Master of Engineering

# Evaluation on tool wear rate and accuracy of patterns in micro prismatic end-milling

by


Ju Eun An

Department of Mechanical Engineering

The Graduate School

Pukyong National University



February 24, 2017

# Evaluation on tool wear rate and accuracy of patterns in micro prismatic end-milling
# (마이크로 프리즘 패턴의 엔드밀링에서 공구 마모와 정밀도 평가)

Advisor: Prof. Jae Seob Kwak

by

Ju Eun An

A thesis submitted in partial fulfillment of the requirements for the degree of

Master of Engineering

in Department of Mechanical Engineering, The Graduate School,
Pukyong National University

February 2017

# Evaluation on tool wear rate and accuracy of patterns in micro prismatic end-milling

A dissertation

by

Ju Eun An

Approved by:

(Chairman) Dae Min Kang

(Member) Tae Wan Kim

(Member) Jae Seob Kwak

February 24, 2017

# Contents

List of tables ········ iii

List of figures ········ iv

List of photographs ········ vi

ABSTRACT ········ vii

1. Introduction ········ 1
   1.1 Background of research ········ 1
   1.2 Domestic and international research trend ········ 3

2. Theoretical background ········ 6
   2.1 Micro prismatic end-milling ········ 6
   2.2 Wear of end mill ········ 8
   2.3 Taguchi method ········ 10

3. Experimental setup ········ 12
   3.1 Experimental apparatus ········ 12
   3.2 Measurement of tool wear and pattern accuracy ········ 20

4. Experimental results ········ 27
   4.1 Evaluation on tool wear of end mill ········ 27
   4.2 Evaluation on accuracy of micro prism pattern ········ 36
   4.3 Relation of tool wear and pattern accuracy ········ 46

5. Conclusions ········· 49

감사의 글 ········· 50
REFERENCES ········· 51

# List of tables

Table 3.1 Specifications of micro prismatic end-milling system ·· 15

Table 3.2 Specifications of micro end mill ································· 16

Table 3.3 Machining Conditions ················································ 16

Table 3.4 Chemical composition(wt.%) of STD-11 ······················ 17

Table 3.5 Mechanical properties of STD-11 ································ 17

Table 3.6 Taguchi $L_9(3^2)$ orthogonal array ································ 18

Table 3.7 Specification of microscope ······································· 22

Table 3.8 Specification of 3D scanner ······································· 26

Table 4.1 ANOVA on wear of micro end mill ······························ 35

Table 4.2 Correlation of tool wear and error on peak ················· 47

# List of figures


Fig. 1.1 Schematic diagram of back light unit ········ 5
Fig. 2.1 Comparison of traditional end-milling system and micro prismatic end-milling system ········ 7
Fig. 2.2 Wear of micro end mill ········ 9
Fig. 3.1 Dimensions of micro prism pattern ········ 17
Fig. 3.2 Basic concept of micro prismatic end-milling ········ 19
Fig. 3.3 Definition of flank wear on micro end mill ········ 23
Fig. 3.4 Definition of boundary wear on micro end mill ········ 23
Fig. 3.5 Example of wear measurement ········ 24
Fig. 3.6 Measurement location of peak to peak and valley to valley distance ········ 25
Fig. 4.1 Width of flank wear at end cutting edge of micro end mill ········ 29
Fig. 4.2 Depth of flank wear at peripheral cutting edge of micro end mill ········ 31
Fig. 4.3 Boundary wear at corner of micro end mill ········ 33
Fig. 4.4 SN ratio on wear of micro end mill ········ 35
Fig. 4.5 Peaks of machined micro prism pattern (x600) ········ 38
Fig. 4.6 Valleys of machined micro prism pattern (x600) ········ 40
Fig. 4.7 Error rate on dimensional accuracy of micro prism pattern ········ 42
Fig. 4.8 Peak and valley of machined micro prism pattern (x1200) 43

Fig. 4.9 Comparison of cutting force in traditional end-milling and micro prismatic end-milling ········································ 47
Fig. 4.10 3D model of experiment No. 3 ································ 48
Fig. 4.11 3D model of experiment No. 7 ································ 48

# List of Photographs

Photo. 3.1 Apparatus of micro prismatic end-milling system ······· 14
Photo. 3.2 Used micro end mill ······························································· 15
Photo. 3.3 Apparatus of video microscope system ························ 22
Photo. 3.4 Apparatus of surface profiler ········································ 26

# 마이크로 프리즘 패턴의 엔드밀링에서 공구 마모와 정밀도 평가

안 주 은

부 경 대 학 교 대 학 원 기 계 공 학 과

**ABSTRACT**

마이크로 프리즘 패턴은 광학 및 디스플레이 산업에서 반사율 증가 등의 효과를 얻기 위해 적용되는 마이크로 패턴의 한 종류이다. 현재 마이크로 패턴의 제작은 주로 리소그래피, 플레이닝, EDM 등의 방법을 통해 이루어지고 있으나 생산비용 및 생산성의 제한이 있다. 초정밀 금형을 사용한 제품생산은 기존 가공법의 단점을 보완할 수 있는 방법으로 산업계가 요구하는 높은 생산성을 보장하는 것이 가능하다. 본 논문에서는 마이크로 엔드밀을 사용하여 금형강인 STD-11에 패턴을 가공하기 위한 방법으로 마이크로 프리즘 엔드밀링을 제안하였다. 이를 통해 BLU의 프리즘 시트에 적용되는 프리즘 패턴을 제작하였다. 또한 가공 후 엔드밀의 플랭크 마모와 경계 마모 정도를 측정하고 실험계획법과 ANOVA를 통해 공구의 마모에 대한 절삭조건의 영향력을 파악하였다. 또한 가공된 패턴의 피크 및 골간 간격을 측정하여 패턴의 치수 정밀도 및 가공 시 발생하는 결함들을 확인하였다. 그 결과 공구의 마모와 패턴의 결함을 최소화할 수 있는 절삭조건을 확인할 수 있었다.

# 1. Introduction

## 1.1 Background of Research

Micro patterning is a technology for machining the pattern with micro size on the surface of products in order to obtain additional functions such as super-hydrophobicity, hydrophilicity, enhancement of luminance, and etc. It has widely been applying to various industries; optics, medicine, aerospace, automobile.[1~5] Micro patterns are mainly fabricated by lithography, laser machining, ultrasonic machining, and electro discharge machining in order to directly manufacture the products. However these processes have disadvantages which are relatively longer production time, limitation of machinable materials, and so forth. Therefore it makes hard that these processes are applied to the mass production. High precision mold is one of the tools to substitute above-mentioned processes, which could assure high productivity required in various industries. Micro machining is one of the proper ways to fabricate high precision mold, and also has advantages, less limitation of machinable materials and fast machining time, which assures high productivity.[6~8]

Especially in the display device industry, precision mold has introduced mass production and enlargement of prism sheet which is the component for enhancement of luminance and light wight in back light unit(BLU), main part of light emitting diode(LED) and liquid crystal display(LCD) display panel.[9] Many studies have focused on the shaping, and planing in order to product the high precision mold with prism patterns, or enhance the efficiency of the pattern. However there are few studies on prism pattern fabricated by micro machining.

Thus in this investigation, micro prismatic end-milling was suggested in order to machine the 100μm of prism pattern on STD-11, the mold metal, with micro flat end mill. Measurement of flank and boundary wear on micro end mill after machining was conducted, and at the same time the effect of cutting parameters were evaluated by design of experiment and analysis of variance(ANOVA). Also the dimensional accuracy and the quality of micro prism pattern were analyzed to derive optimal cutting condition.

## 1.2 Domestic and International Research Trend

Micro prism pattern focused on optics and disply industry is applied to the prism sheet in back light unit of LCD, LED panel, camera lens for streoscopic observation, display of virtual keyboard, and so forth.[10~12]

In recent, many researches are focused on the fabrication of micro prism pattern and its performance. Deng et al.[13] developed symmetric prism pattern in order to get 3D photography with micro prism single lens. With simulation and experimentation, 3D photography was obtained with one air-photo remote camera. Funamoto et al.[14] designed double prism pattern to light weighting of back light unit and increase its efficiency. Developed pattern was adapted to the reflective sheet and it replaced diffusive sheet and two prism sheet in back light unit(BLU).

Studies on the precision mold with micro pattern have conducted in order to satisfy the requirements of industry; weight lightening, enlargement, high-precision and etc. Park et al.[15] machined micro prism pattern on aluminium alloy with diamond tool, and analyzed dimensional accuracy of pattern, its quality, and the tool wear. They minimized the wear on tool, and determined the most influence factors on tool wear. Yoo et al.[16] fabricated prism pattern on polymethyl methacrylate(PMMA) plate by injection mold. A mold was designed to decrease injection defects and secure the precision and quality of products.

BLU is one of the main parts in display device, which has the role to change the light from light sources into the flat light having regular luminance. It is applied to many display products like TV, monitor, smart phone, and so forth.[17] Fig. 1.1 shows its basic structure consisted with mold frame, reflector sheet, light guide panel, LED, diffuser sheet, prism sheet, protector sheet. In general display panel, back light unit spends 30~50% of power consumption, so development of high efficiency BLU is required to improve its performance.[18~21]

The researches have tended to focus on the fabrication of micro prism pattern and its performance, rather than on machining of mold for mass production or its accuracy and efficiency. Thus in this paper, micro prism pattern was machined on mold metal and its quality was evaluated.

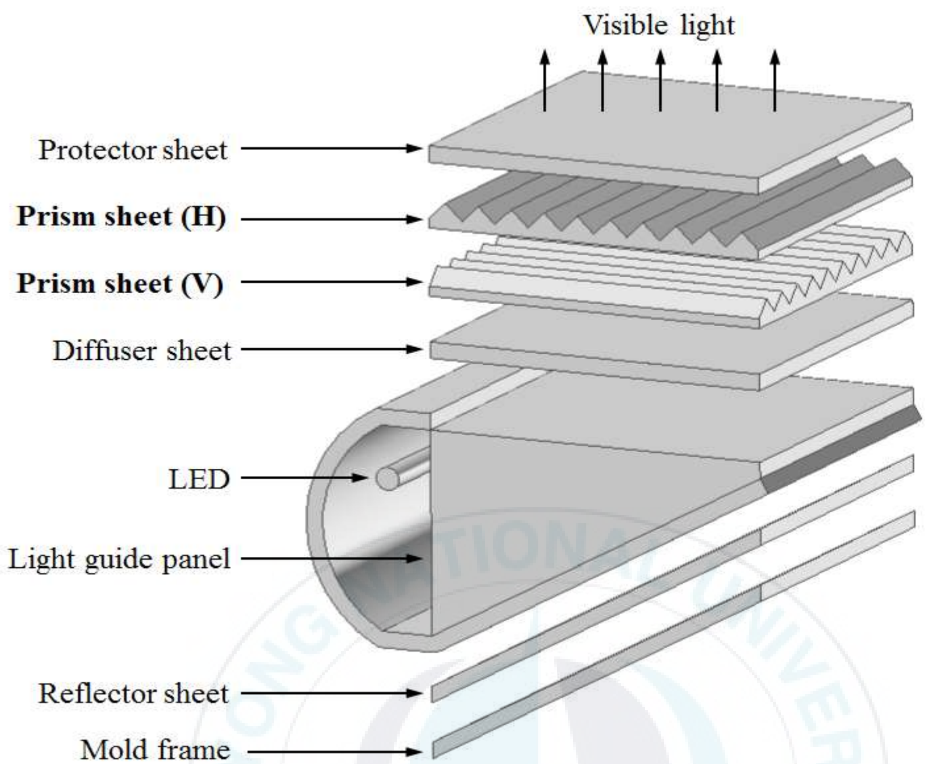


Fig. 1.1 Schematic diagram of back light unit

# 2. Theoretical Background

## 2.1 Micro Prismatic End-Milling

Most of mold having micro pattern is fabricated by lithography, shaper, and planer, but these ways have lower productivity owing to relatively longer processing time and increase of machining error. Hence they are hard to satisfying the requirements of the industry. Not only shaper and planer need diamond cutting tool, but the unit cost of production rises. Thus securement of machining process with high productivity and low unit cost of production is required.

This paper suggests micro prismatic end-milling in order to replace above-mentioned processes. As shown in Fig. 2.1 (a), machined surface and end mill are perpendicular in traditional micro end-milling. On the other hand, the surface and the tool have certain angle smaller than 90° in micro prismatic end-milling as Fig. 2.1 (b) represents. With this machining system, it is possible to remove triangular cross section with flat end mill.

As one of advantages, this process is able to utilize traditional end-milling apparatus and knowledge, whereas lithography or planing are not. Also it has relatively short machining time, less limitation of machinable materials, and lower unit cost due to use cheaper tools. However in micro prismatic end-milling, the tool receives cutting force only one side, so it could make both deformation of tool and machining error. Thus it is need to evaluate the effect of machining parameters on tool and pattern, in order to reduce defects of product and increase the dimensional accuracy.

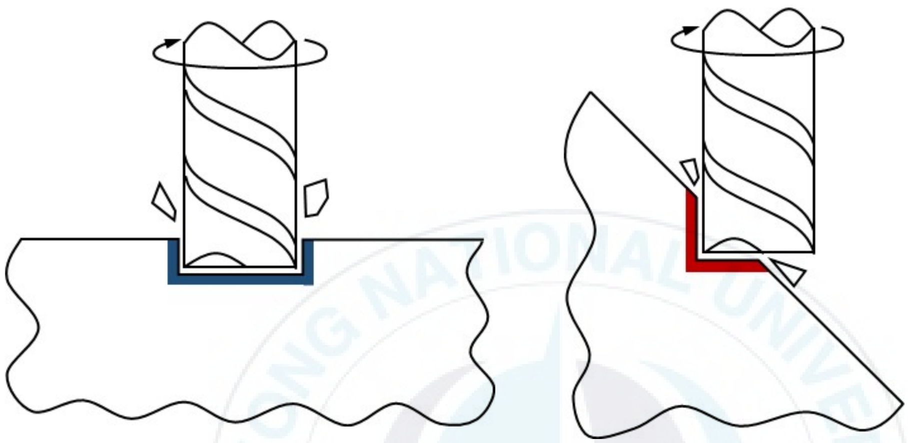

(a) Traditional micro end-milling (b) Micro prismatic end-milling

Fig. 2.1 Comparison of traditional end-milling system and micro prismatic end-milling system

## 2.2 Wear of End Mill

In the cutting process, the wear of tool is one of the important factors, which affect tool life, dimensional accuracy of products, surface roughness, hardness, and so on.(22) As shown in Fig. 2.2, he wear is divided as three by its location, which are crater wear, flank wear, and boundary wear. Crater wear is generated in a tool face by the friction at chip-tool interface, which has shape of crater. It has less influence on the product than other wears because it located little off from the edge of tool. However it could induce fracture of tool when the crater wear increases due to continuous machining. Flank wear is generated by the friction in flank face. It rapidly grows when the cutting speed is excessively fast or slow. This wear could decrease the tool life, and at the same time affect accuracy of product. Especially in micro machining that requires high precision, small amount of flank wear could make large effect on the products. Boundary wear between flank face and tool face is generated by impact when the tool entered into the workpiece. It increases nose radius and decreases tool diameter, which means it also affects dimensional accuracy of products.

In micro machining, small wear could make large defects on products. Thus it needs to find the machining conditions for minimizing the tool wear in order to secure the both quality and productivity.(23)

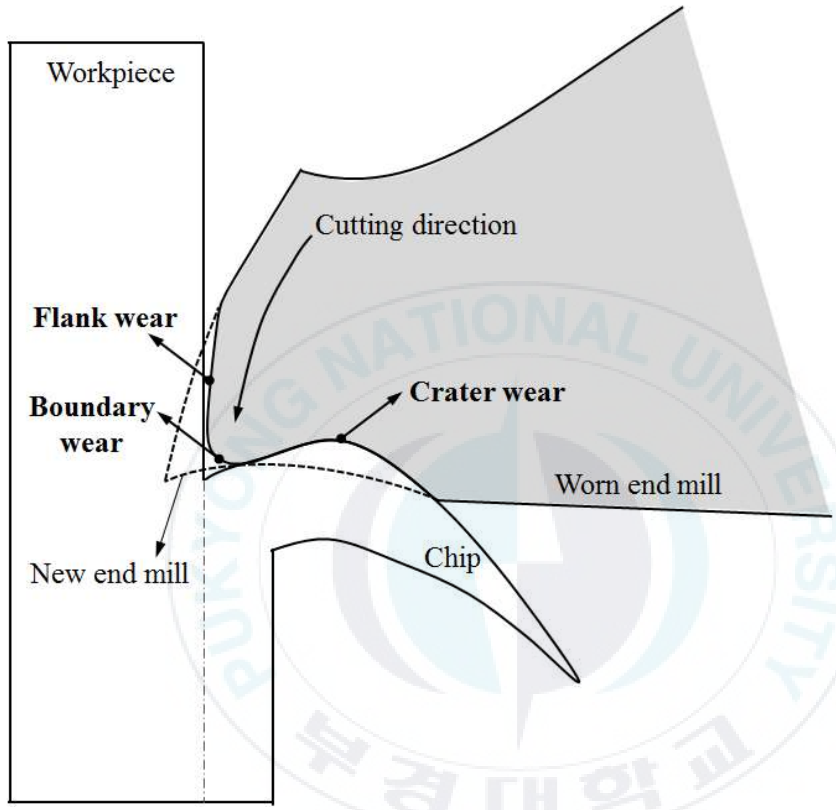

Fig. 2.2 Wear of micro end mill

## 2.3 Taguchi Method

Taguchi method is a quality assurance method developed by Genichi Taguchi in Japan, which evaluates quantitative influence of both controllable internal factors and uncontrollable external factors or hard to control parameters at the same time.[24] This method has numerical evaluation on external factors called noise factors to determine its influence. Also quality deviation is demonstrated as the loss function that shows extent of the difference between the characteristics value and the target value. The loss functions in Taguchi method are divided by smaller-the-better characteristic, larger-the-better characteristic, and nominal-the-best characteristic.

Smaller-the-better characteristic selected in this investigation represents the case that smaller characteristics value means the better product quality. The equation of loss function *L(y)* in this case is in Eq. (1).

$$\begin{aligned} L(y) &= ky^2 \\ &= \frac{A}{\Delta^2}y^2 \end{aligned} \tag{1}$$

where $y$ is measured value, $k$ is constant, $A$ is loss, and $\Delta$ is acceptable limit.

In Taguchi method, signal to noise(SN) ratio is derived in order to minimize the effect of uncontrollable factors, and the controllable factors able to reduce quality change are figured out. SN ratio is calculated with following Eq. (2).

$$\text{SN ratio} = \frac{\text{power of signal}}{\text{power of noise}} = \frac{\text{estimate of square of population mean}}{\text{estimate of variance}} \tag{2}$$

Combining Eq. (1) and Eq. (2), SN ratio in smaller-the-better characteristics is derived as Eq. (3).

$$SN = -10\log\left[\frac{1}{n}\sum_{i=1}^{n} {y_i}^2\right] \tag{3}$$

where y is measured value, n is number of experimentation, and larger SN ratio means the combination of factors less affected by noise factors.

# 3. Experimental Setup

## 3.1 Experimental Apparatus

In this investigation, the determination on flank and boundary wear of micro end mill in various machining conditions was conducted with micro prismatic end-milling. Dimensional accuracy of fabricated micro prism pattern and defections like burr were also evaluated. Photo. 3.1 shows micro end-milling system which consists integrated multi-process CNC machine(Hyper-15, Hybrid Precision), spindle, and jig. Magnified photography at bottom shows the micro flat end mill and the workpiece tilted 45°. Specifications of multi-process CNC machine and spindle are represented in Table 3.1. Micro flat end mill(4G Mills, YG1) having 300μm of diameter and 2 flutes is shown in Photo. 3.2, and its specifications are represented in Table 3.2.

To determine the machining characteristics in micro prismatic end-milling, spindle speed and feed rate were selected as machining parameters. Table 3.3 represents machining parameters and fixed conditions in this experimentation. Material of workpiece is STD-11, spindle speeds are 15000, 17500, 20000rpm, and feed rates are 20, 30, 40mm/min based on recommended by a tool supplier as cutting conditions of micro end mill. Depth of cut was fixed as 5μm and lubricant was not used in whole experimentations. Chemical composition and mechanical properties are represented in Table 3.4 and Table 3.5.

Fig. 3.1 shows the size of fabricated micro prism pattern of which pitch and height is 100µm, angle is 90°, and length is 5mm. The size of pattern is based on the requirements of industries.[25] Table 3.6 represents the orthogonal array($L_9 3^2$) based on Taguchi method. Each experimentation was carried out with new end mill.

Fig. 3.2 indicates basic concept of micro prismatic end-milling process in this experimentations. As the tool path in figure describes, end mill moves 5µm, depth of cut, in +y direction, and fabricates the pattern to move 5mm in +x direction. After machining it moves as depth of cut in −y direction and return to the point where machining starts. This processes are repeated until the end of machining.

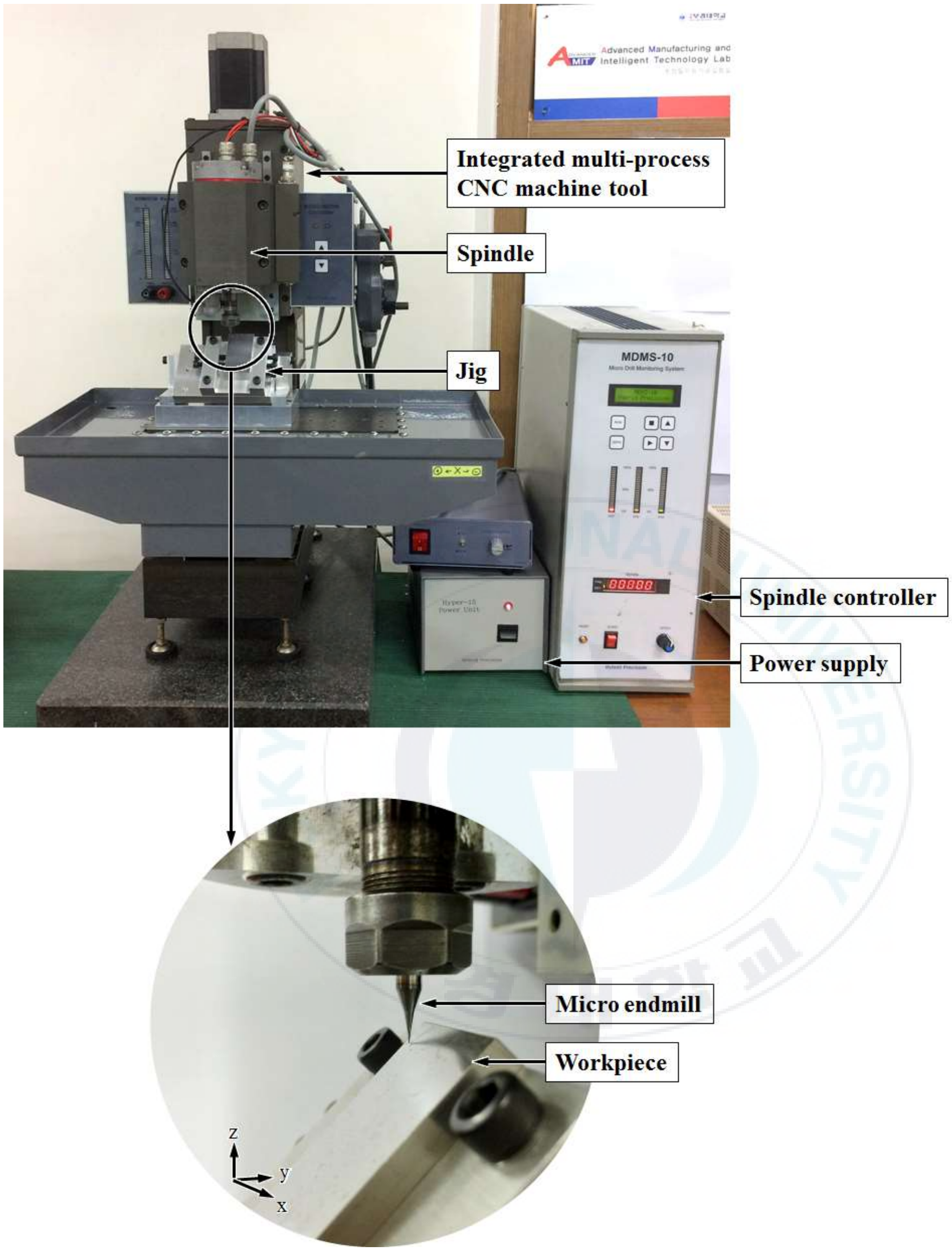


Photo. 3.1 Apparatus of micro prismatic end-milling system

Table 3.1 Specifications of micro prismatic end-milling system

| Items | Specification |
| --- | --- |
| Spindle velocity (rpm) | 1,000 ~ 23,000 |
| Movement length of X axis (mm) | 130 |
| Movement length of Y axis (mm) | 75 |
| Movement length of Z axis (mm) | 80 |
| X, Y, Z axis resolution (μm) | 0.1 |
| X, Y, Z axis feed rate (mm/min) | 0.01 ~ 400 |

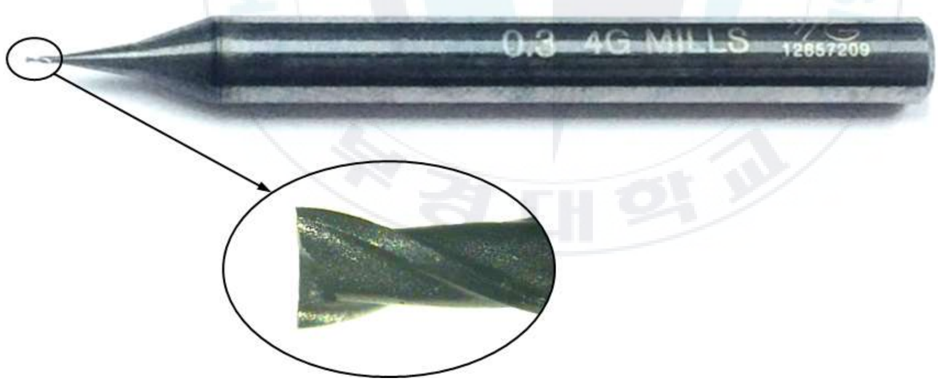


Photo. 3.2 Used micro end mill

Table 3.2 Specifications of micro end mill

| Items | Specification |
|---|---|
| Tool diameter (μm) | 300 |
| Length of cut (μm) | 600 |
| Helix angle (°) | 30 |
| Shank diameter (mm) | 4 |
| Flute | 2 flutes |
| End mill type | Flat |
| Tool material | Micro grain carbide |

Table 3.3 Machining Conditions

| Items | Value |
|---|---|
| Material | STD-11 |
| Spindle speed (rpm) | 15000, 17500, 20000 |
| Feed rate (mm/min) | 20, 30, 40 |
| Depth of cut (μm) | 5 |
| Lubrication | Dry cutting |

Table 3.4 Chemical composition(wt.%) of STD-11

| | C | Si | Mn | P | S | Cr | Mo | V | Fe |
|---|---|---|---|---|---|---|---|---|---|
| STD-11 | 1.57 | 0.30 | 0.40 | 0.025 | 0.003 | 12.05 | 1.00 | 0.44 | 84.21 |

Table 3.5 Mechanical properties of STD-11

| Items | Value |
|---|---|
| Tensile strength (MPa) | 231 |
| Yield strength (MPa) | 154 |
| Hardness (HRC) | 30 |

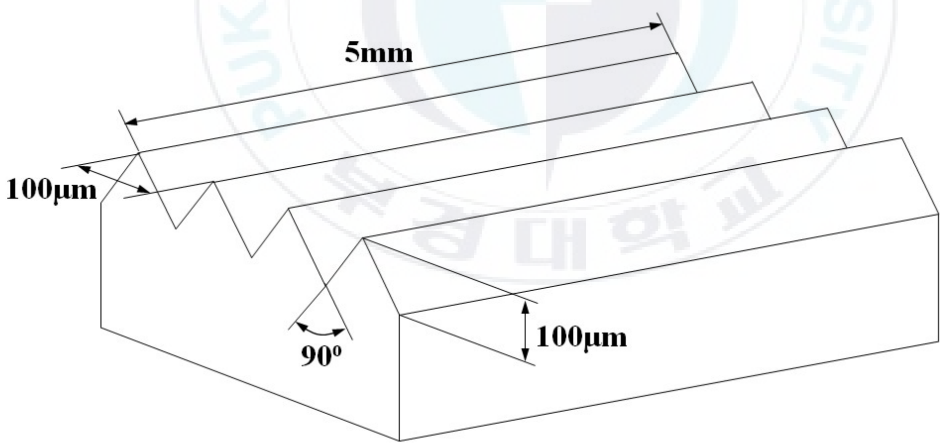


Fig. 3.1 Dimensions of micro prism pattern

Table 3.6 Taguchi $L_9(3^2)$ orthogonal array

| No. | Spindle speed (rpm) | Feed rate (mm/min) |
|---|---|---|
| 1 | 15,000 | 20 |
| 2 | 15,000 | 30 |
| 3 | 15,000 | 40 |
| 4 | 17,500 | 20 |
| 5 | 17,500 | 30 |
| 6 | 17,500 | 40 |
| 7 | 20,000 | 20 |
| 8 | 20,000 | 30 |
| 9 | 20,000 | 40 |

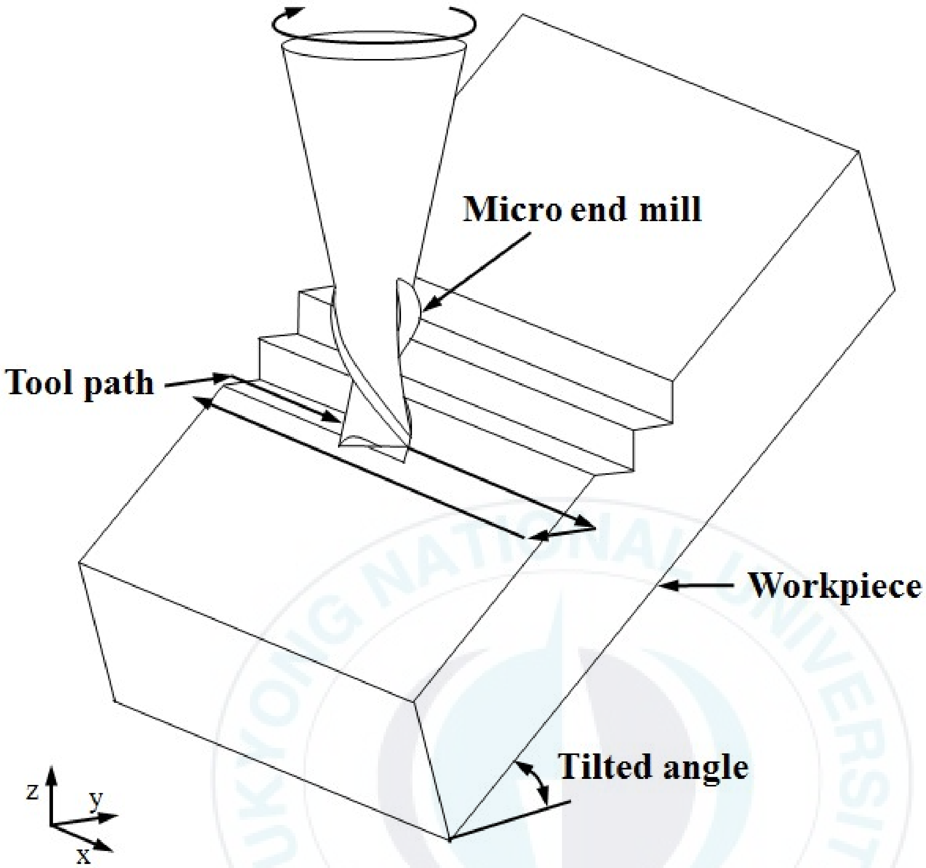


Fig. 3.2 Basic concept of micro prismatic end-milling

## 3.2 Measurement of tool wear and pattern accuracy

Measurement of both tool wear and accuracy of pattern was carried out with video microscope system. The microscope(SV-35, Sometech) and its stored program(ITPlus4.0) are shown in Photo. 3.3, and its specification is represented in Table 3.7. Before evaluating the wear of micro end mill, it was needed to define the criterion of tool wear. Flank wear and boundary wear which have influence on accuracy of products were measured and evaluated by defined criteria.

Fig. 3.3 and Fig. 3.4 indicate the measurement criteria of flank wear and boundary wear, respectively. As Fig. 3.3 shows, flank wear was measured in 2 ways because cutting process is conducted at both end cutting edge and peripheral cutting edge in end mill. Flank wear is generated in both cutting edge of end mill, so the maximum wear in end cutting edge is defined as width of flank wear, and the maximum wear in peripheral cutting edge is defined as depth of cutting edge. Fig. 3.4 indicates the criterion of boundary wear. As machining progresses, radius of corner increases due to the wear. Thus radius difference at corner is defined as boundary wear. Fig. 3.5 indicates the example of wear measurement on used micro end mill based on defined measurement criterion.

Fig. 3.6 represents the measurement location at machined micro prism pattern in order to analyze the accuracy. To secure the reliability of data, measurement was conducted in three parts, beginning(①), middle(②), and end(③) part of machining. Peak to peak and valley to valley distance were measured three times, and its error rate was calculated with following Eq. (4).

$$\text{Error rate} = \frac{|\text{Measured value - Theoretical value}|}{\text{Theoretical value}} \times 100 \ \ (\%) \quad (4)$$

Photo. 3.4 shows the apparatus of surface profiler(New View 7300 System, Zygo Corp.) used to get 3D model of pattern and Table 3.8 represents its specification.

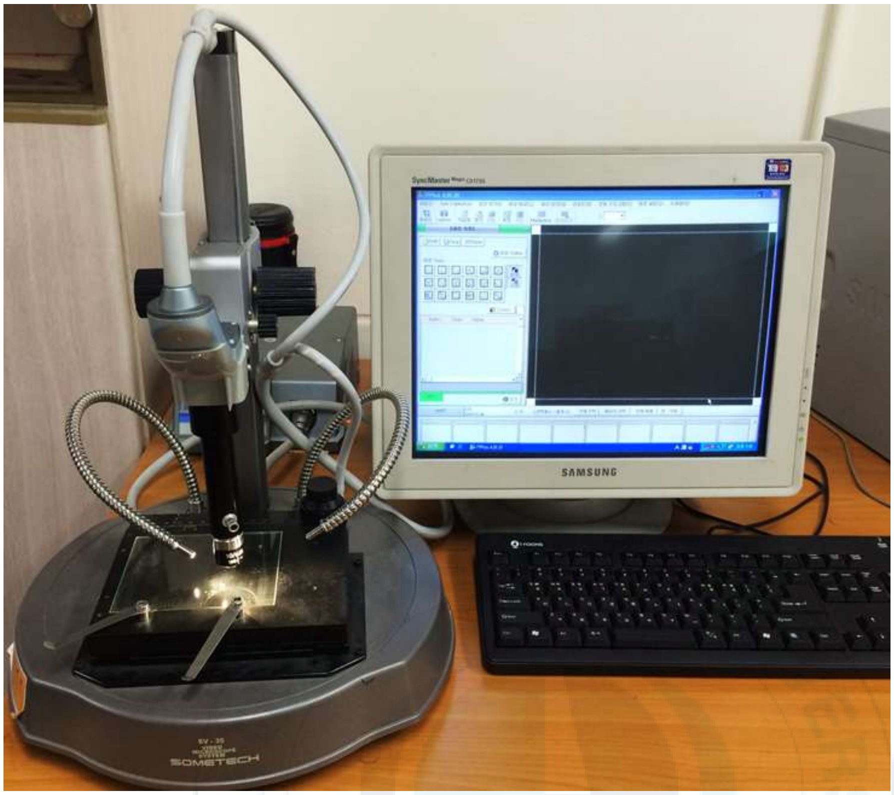


Photo. 3.3 Apparatus of video microscope system

Table 3.7 Specification of microscope

| Item | Specification |
|---|---|
| Image sensor | 1/2.9″ CMOS(2.1M Pixel) |
| Effective pixels | 1920x1080 |
| Cable length | 2M |
| Light source | 35W white LED/5700K<br>150W Halogen |
| Light intensity | 10 level |

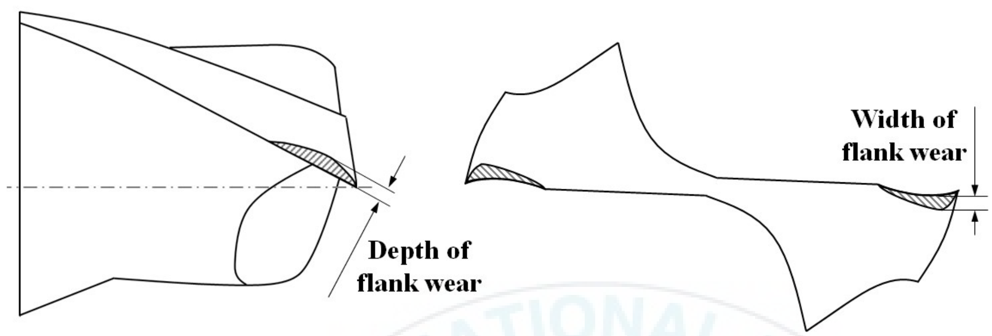


Fig. 3.3 Definition of flank wear on micro end mill

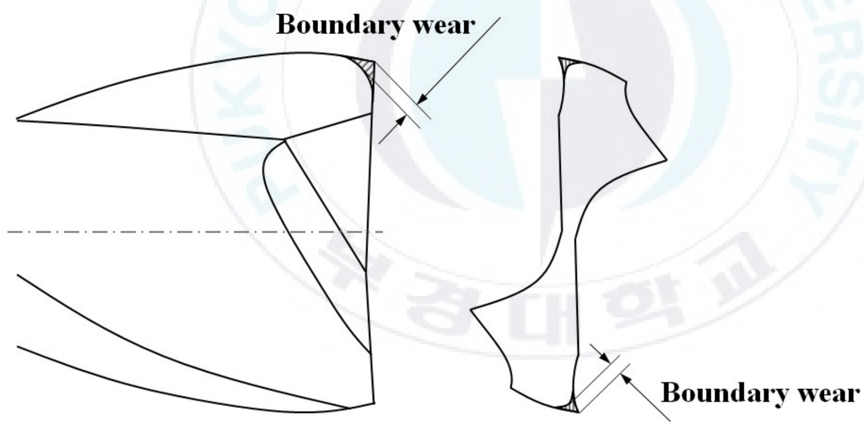


Fig. 3.4 Definition of boundary wear on micro end mill

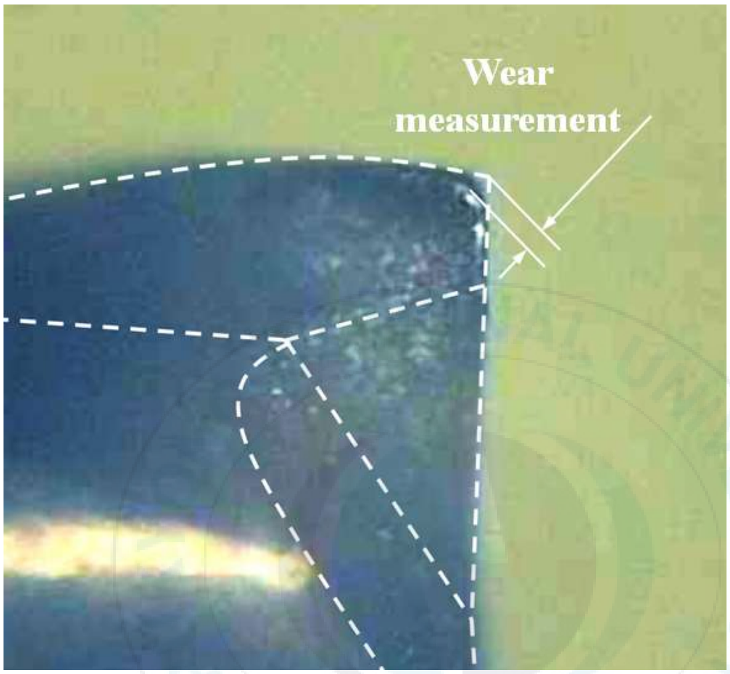


Fig. 3.5 Example of wear measurement

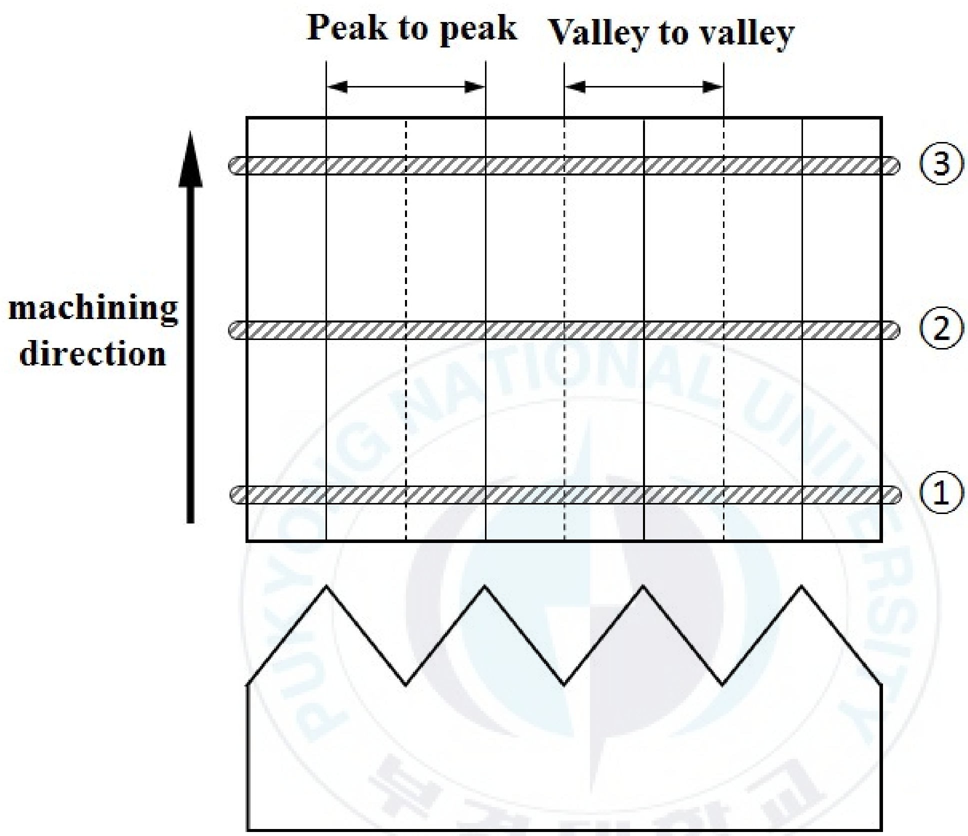


Fig. 3.6 Measurement location of peak to peak and valley to valley distance


Photo. 3.4 Apparatus of surface profiler

Table 3.8 Specification of surface profiler

| Item | Specification |
| --- | --- |
| Vertical scan length | 150 μm |
| Vertical resolution | 0.1 nm |
| Horizontal resolution | 0.36 ~ 9.5 μm |
| Data scan rate | 135 μm/s or more |
| Maximum data points | 307, 200 |

# 4. Experimental Results

## 4.1 Evaluation on Tool Wear of End Mill

In this paper, prism pattern was fabricated with micro prismatic end-milling and the effect of cutting parameters on flank wear and boundary wear was evaluated.

Fig. 4.1 shows 600 times magnified end cutting edge of tool before and after machining taken with metallographic microscope, which shows the width of flank wear. (a) is the micro end mill before machining and (b)~(d) are the tools having larger wear than other conditions when spindle speed is 15,000rpm. When spindle speed is 20,000rpm and feed rates are 20, 30, 40mm/min, the tool has the flank wear as (h)~(j). In experiment no. 7(Fig. 4.1 (h)), the end mill has the minimum width of flank wear, 11.77μm, because it has smallest material per tooth. However the maximum width of flank wear was measured in experiment no. 3(Fig. 4.1 (d)) when spindle speed and feed rate are 15,000rpm and 40mm/min, respectively. Depth of flank wear is represented in Fig. 4.2, 600 times magnified peripheral cutting edge of micro end mill. Fig. 4.2 (a) shows the peripheral edge before machining. When spindle speed is 15,000rpm, depth of flank wear was averagely larger than other conditions because it has longer cutting time per tooth. Relatively lower spindle speed could increase the amount of removed material per tooth, and generate larger frictional force on flank face of tool. In experiment no. 3(Fig. 4.2 (d)), the end mill has the largest depth of flank wear, 27.03µm, among the all experimentations, and also chipping occurred at the cutting edge. While the minimum depth of flank wear was measured at experiment no. 7, 9.19µm. Fig. 4.3 represents boundary wear at corner of micro end mill magnified 600 times. Fig. 4.3 (a) shows the tool before machining, and (b)~(j) show the tool after machining with various conditions. Fig. 4.3 (d) has largest wear which was 8.06µm, and (h) shows the smallest wear like the results of flank wear, 5.24µm.

Comparing whole results of experimentation, micro end mill has the largest wear when spindle speed is 15,00rpm and feed rate is 40mm/min. This is the combination of slowest spindle speed and fastest feed rate in this experimentations, so it has larger material per tooth and higher cutting force. When spindle speed and feed rate are relatively 20,000rpm and 20mm/min, however both flank wear and boundary wear has the minimum value with small material per tooth and lower cutting force.

When the tool wear decreases, tool life increases and at the same time the unit cost of production decreases. Thus signal to noise ratio of smaller-the-better characteristics in Eq. (3) was calculated on wear of micro end mill. SN ratios on two machining factors are represented in Fig. 4.4. SN ratio is proportional to the increase of spindle speed, and decrease of feed rate. Table 4.1 indicates analysis of variance(ANOVA) on the tool wear and it shows that feed rate is statistically significant in 90% of confidence level. Coefficient of determination($R^2$) of ANOVA is 94.5%.

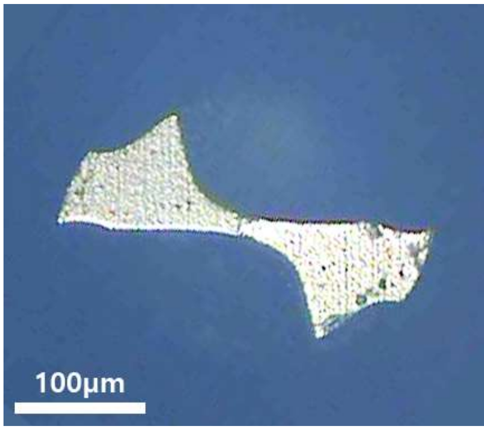


(a) Before machining

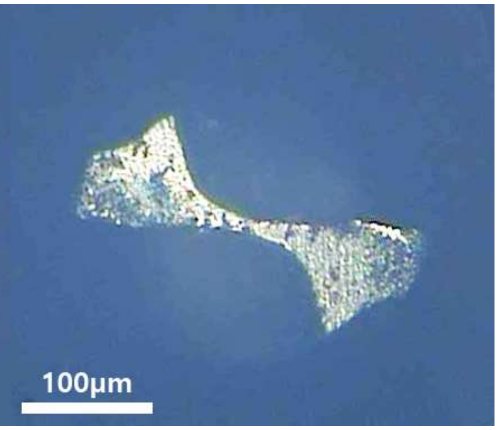


(b) No. 1
(Spindle speed 15,000rpm, Feed 20mm/min)

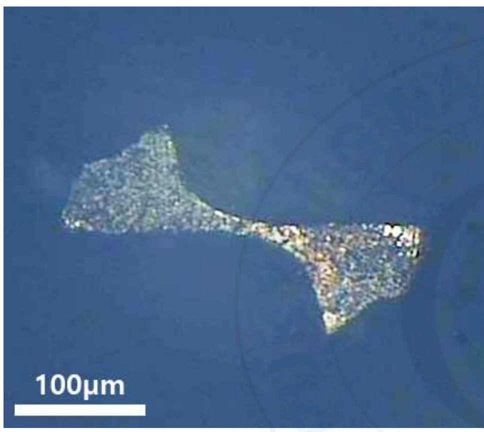


(c) No. 2
(Spindle speed 15,000rpm, Feed 30mm/min)

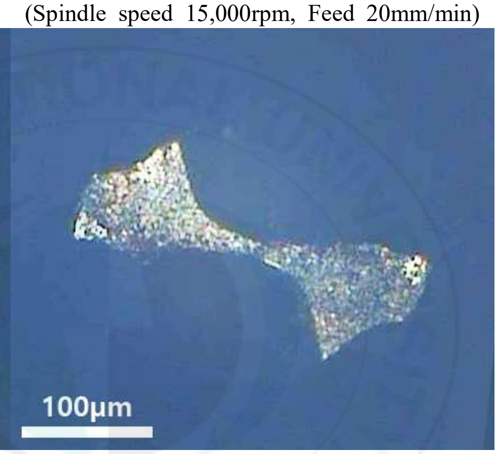


(d) No. 3
(Spindle speed 15,000rpm, Feed 40mm/min)

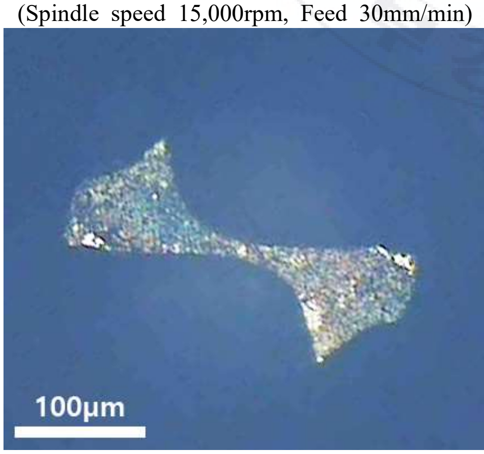


(e) No. 4
(Spindle speed 17,500rpm, Feed 20mm/min)

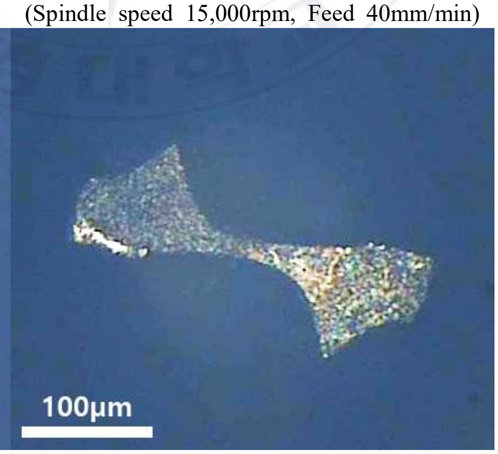


(f) No. 5
(Spindle speed 17,500rpm, Feed 30mm/min)

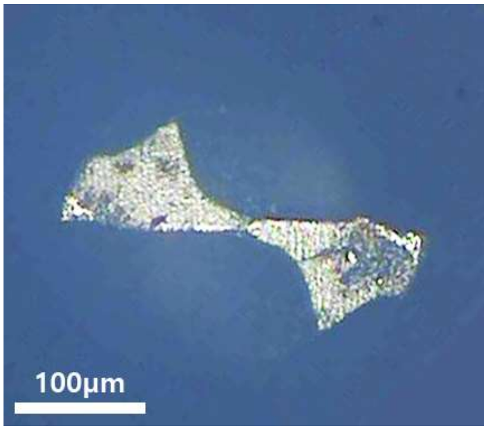


(g) No. 6
(Spindle speed 17,500rpm, Feed 40mm/min)

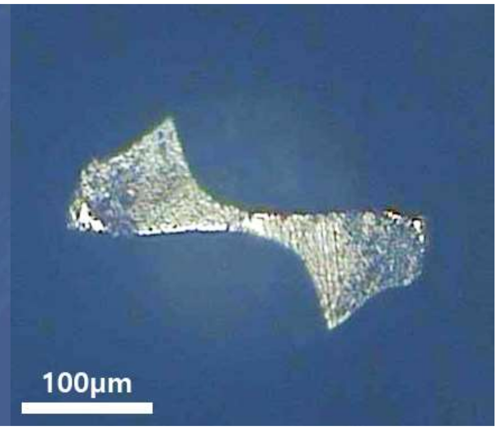


(h) No. 7
(Spindle speed 20,000rpm, Feed 20mm/min)

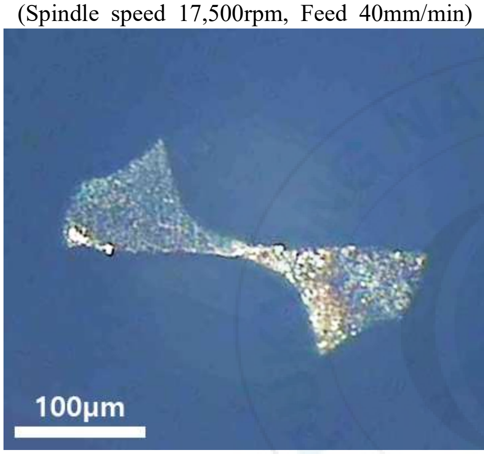


(i) No. 8
(Spindle speed 20,000rpm, Feed 30mm/min)

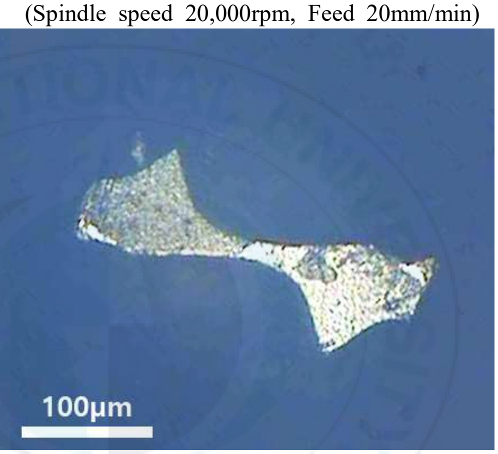


(j) No. 9
(Spindle speed 20,000rpm, Feed 40mm/min)

Fig. 4.1 Width of flank wear at end cutting edge of micro end mill

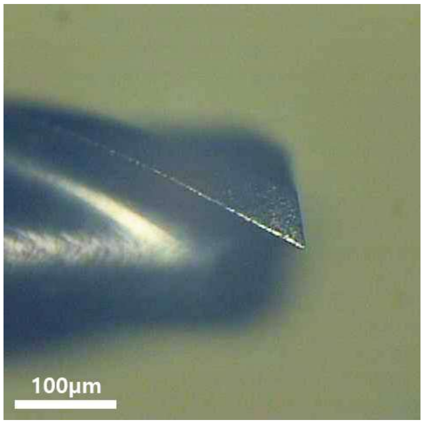


(a) Before machining

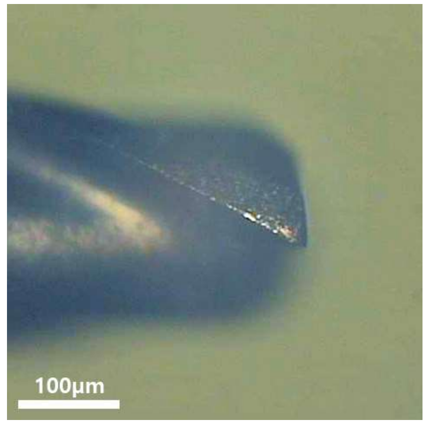


(b) No. 1

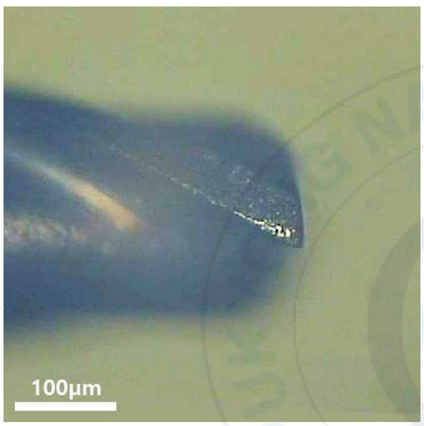


(c) No. 2

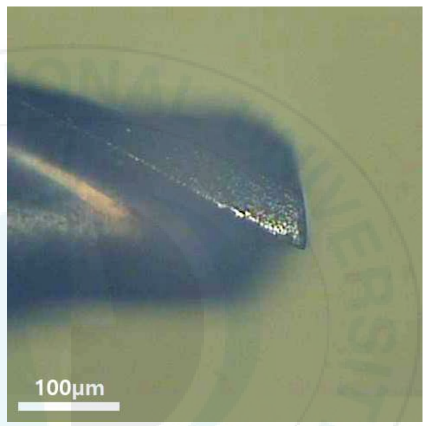


(d) No. 3

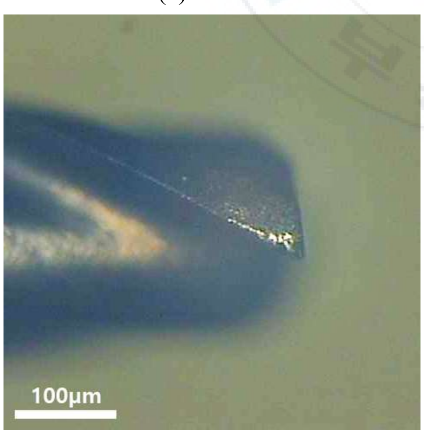


(e) No. 4

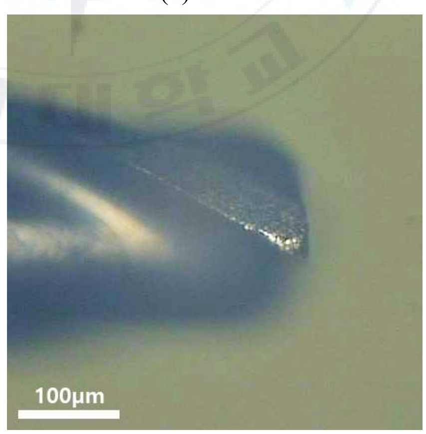


(f) No. 5

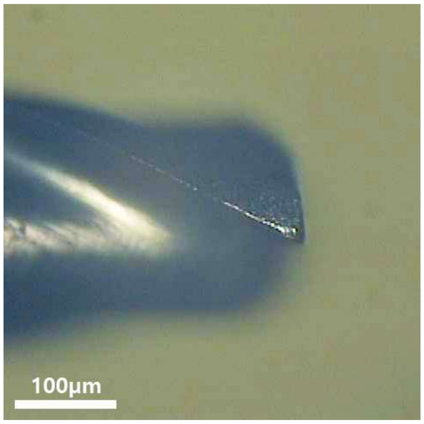


(g) No. 6

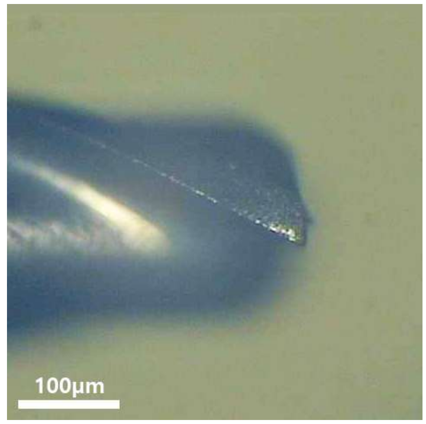


(h) No. 7

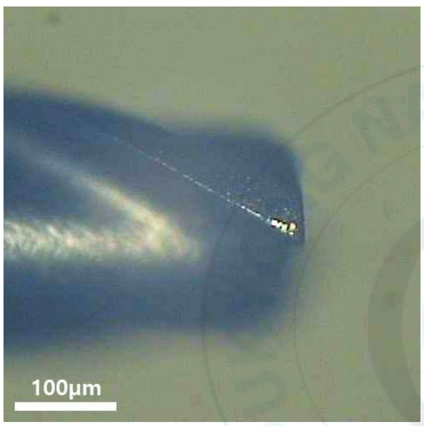


(i) No. 8

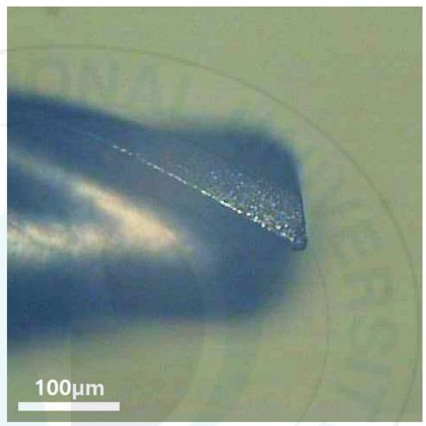


(j) No. 9

Fig. 4.2 Depth of flank wear at peripheral cutting edge of micro end mill

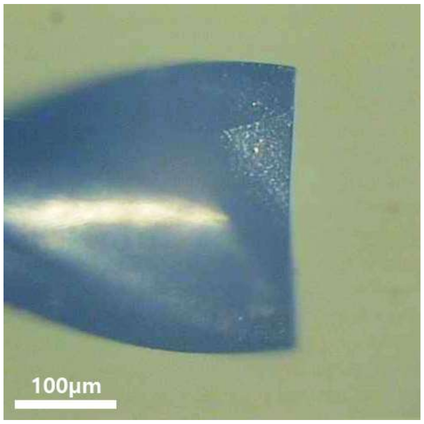


(a) Before machining

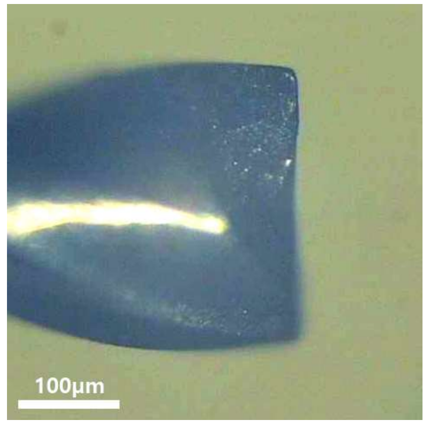


(b) No. 1

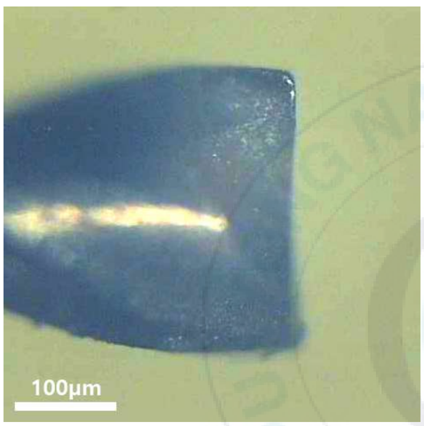


(c) No. 2

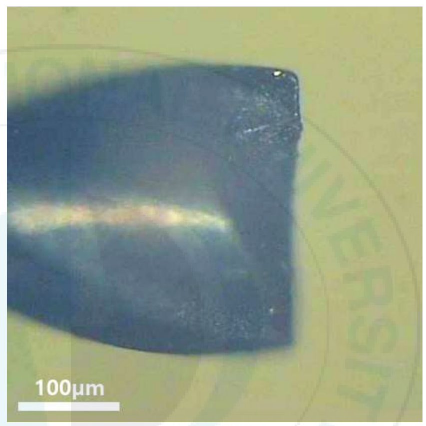


(d) No. 3

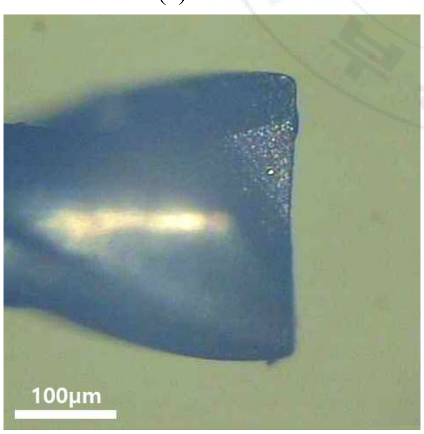


(e) No. 4

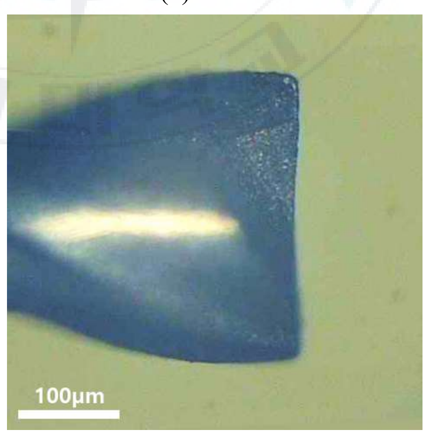


(f) No. 5

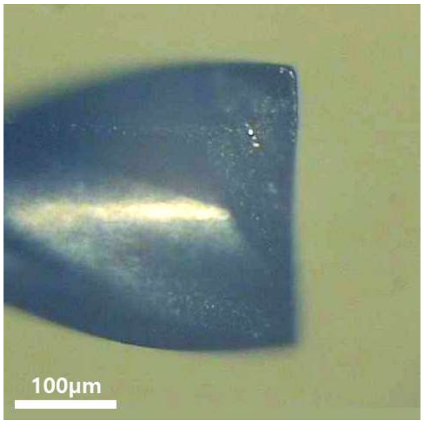


(g) No. 6

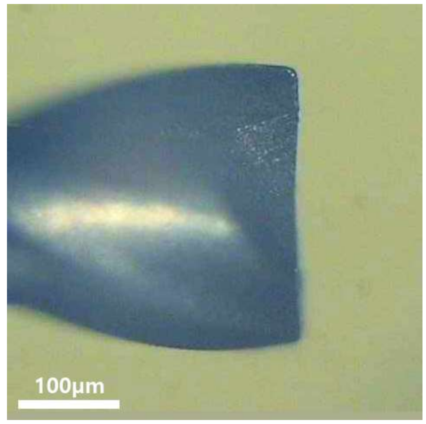


(h) No. 7

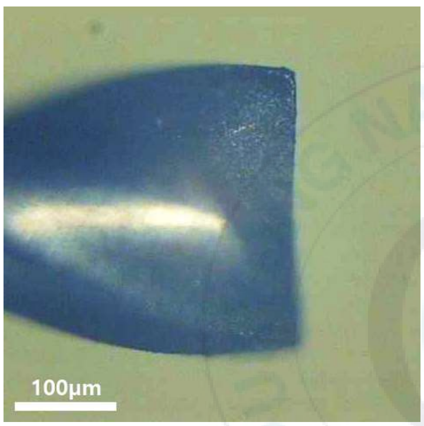


(i) No. 8

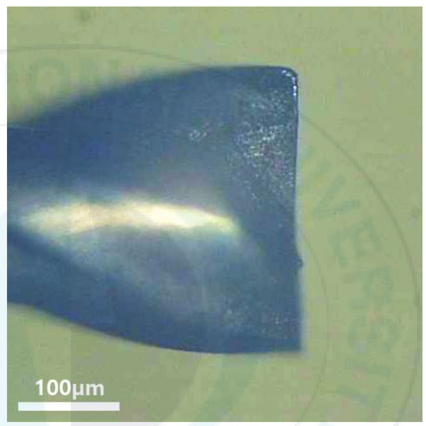


(j) No. 9

Fig. 4.3 Boundary wear at corner of micro end mill

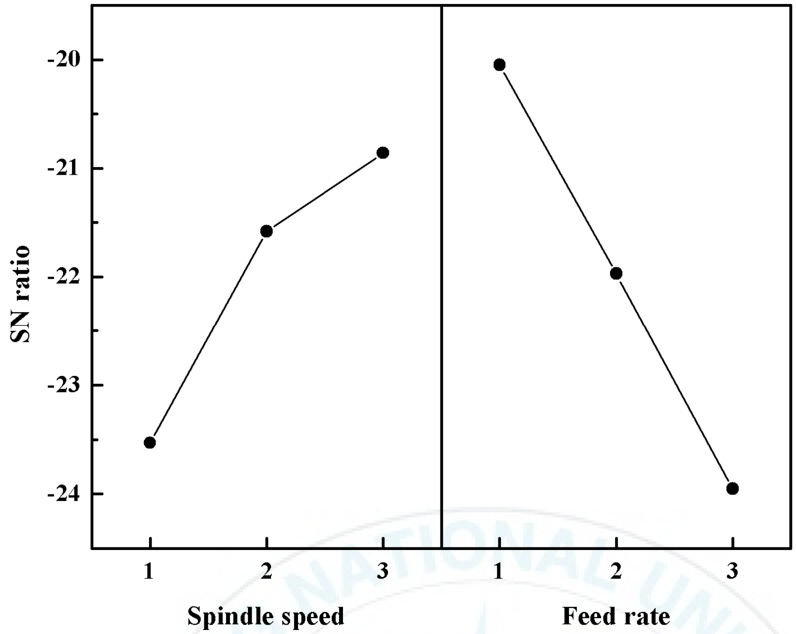


Fig. 4.4 SN ratio on wear of micro end mill

Table 4.1 ANOVA on wear of micro end mill

| Source | DF | SS | MS | F | P |
|---|---|---|---|---|---|
| A | 2 | 11.5092 | 5.7546 | 11.53 | 0.022 |
| B | 2 | 22.7896 | 11.3948 | 22.83 | 0.006 |
| Error | 4 | 1.9964 | 0.4991 | | |
| Total | 8 | 36.2952 | | | |

($R^2$=94.5%)

## 4.2 Evaluation on Accuracy of Micro Prism Pattern

Micro prism pattern having 100μm size was fabricated on STD-11, and its dimensional accuracy and defects were analyzed. Defects and dimensional accuracy were analyzed with photography taken with microscope. Fig. 4.5 and Fig. 4.6 respectively show 600 times magnified peaks and valleys of machined pattern. In (a)~(f), there are some parts to show low straightness due to the vibration, cutting force, and so forth. (g)~(h) relatively show better straightness.

Fig. 4.7 indicates the error rate of peak to peak and valley to valley distance with each machining condition. Experiment no. 8, 20,000rpm of spindle speed and 30mm/min of feed rate, has the maximum error rate. Its error rate of peak to peak distance is 4.27%, and valley to valley distance is 3.09%. On the other hand, the minimum error rate of peak to peak and valley to valley distance are respectively 0.08% and 0.32% when spindle speed is 20,000rpm and feed rate is 40mm/min. Generally valley to valley error was more irregular than peak error, and it is considered that deflection at bottom of tool was larger than upper part of micro end mill as Fig. 2.2 shown.

Fig. 4.8 represents 1200 times magnified peak and valley of micro prism pattern. Length of burrs on peak tended to be proportional to decrease of spindle speed. (a)~(c) in Fig. 4.8 were machined with spindle speed of 15,000rpm and respectively 20, 30, 40mm/min of feed rate, and they have relatively larger burrs on peak and irregular machining on valley. Experiment no. 7 to 9 were carried out with spindle speed of 20,000rpm in each feed rate. They have less burrs and defects than other patterns. Especially experiment no. 9 has little defects on peak and valley. In the industry, to secure the tool life for the unit cost and productivity is important, but fabricating the best quality of product is the first considered requisite. As a result, 20,000rpm of spindle speed and 40mm/min of feed rate are acceptable machining conditions to get the product having better quality in micro prismatic end-milling.

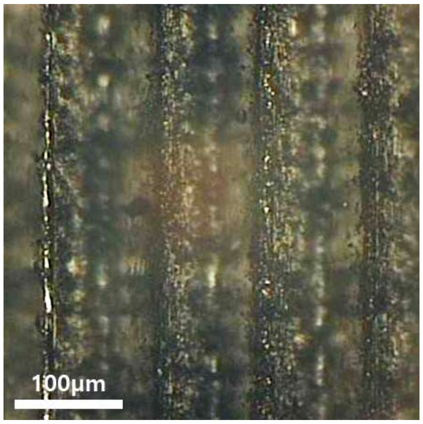


(a) No. 1

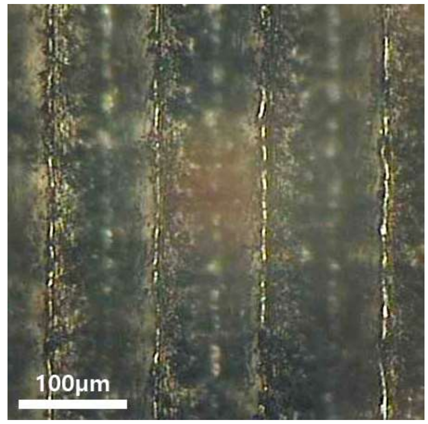


(b) No. 2

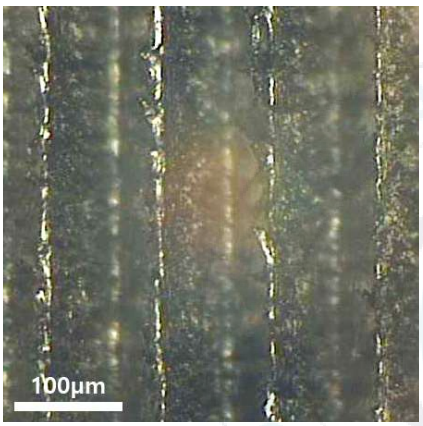


(c) No. 3

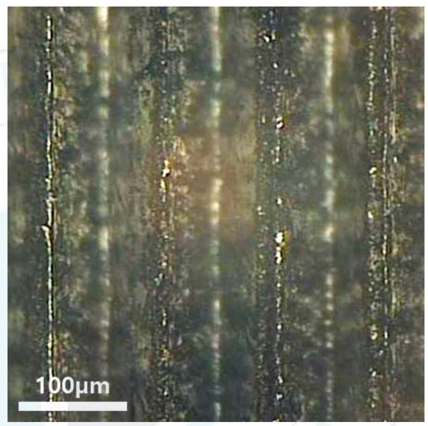


(d) No. 4

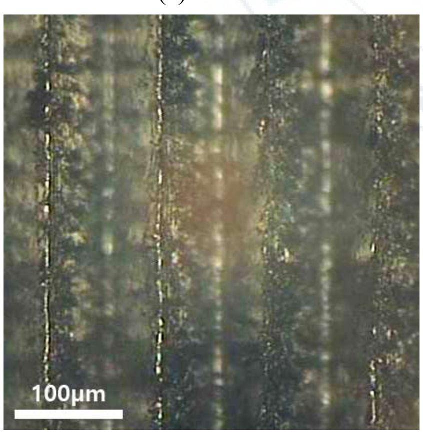


(e) No. 5

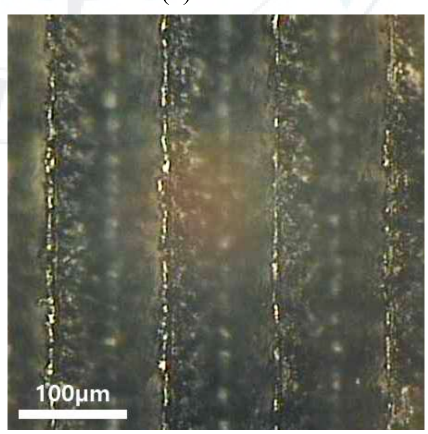


(f) No. 6

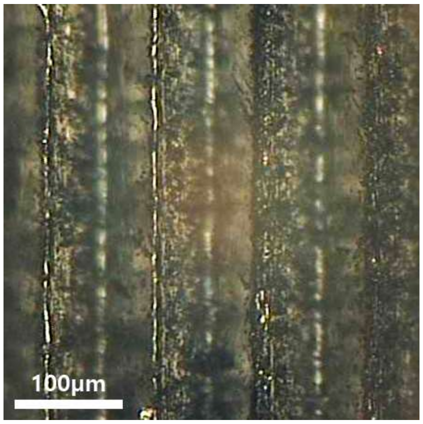


(g) No. 7

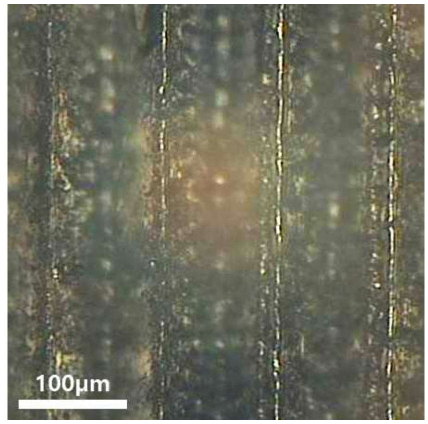


(h) No. 8

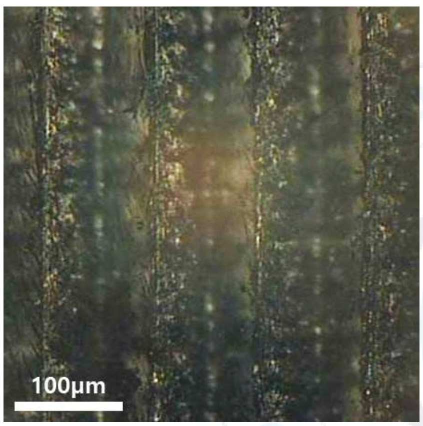


(i) No. 9

Fig. 4.5 Peaks of machined micro prism pattern (x600)

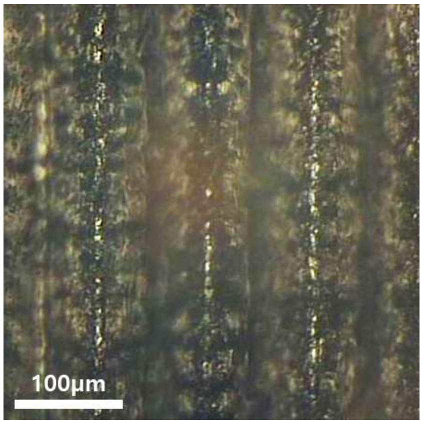

(a) No. 1

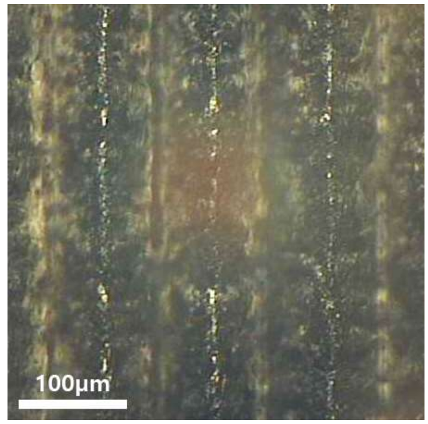

(b) No. 2

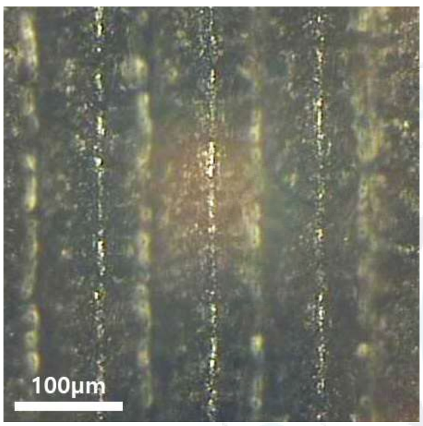

(c) No. 3

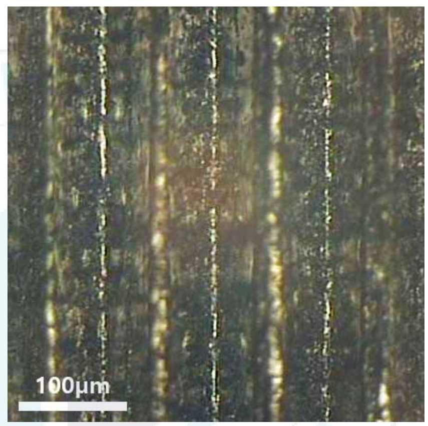

(d) No. 4

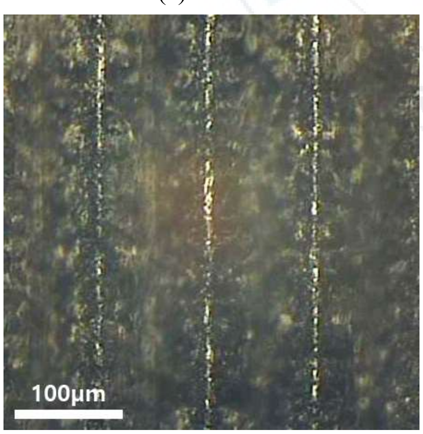

(e) No. 5

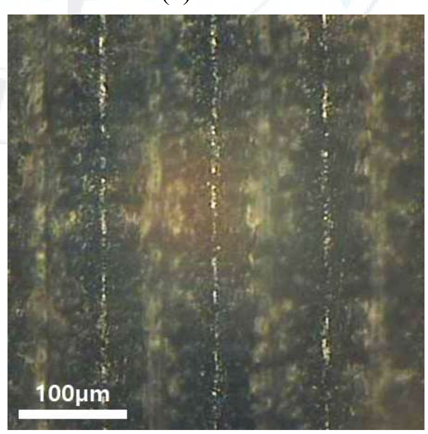

(f) No. 6

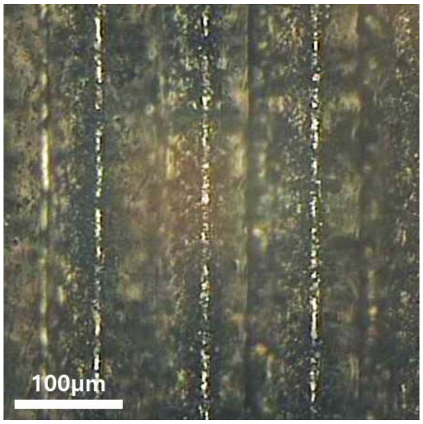


(g) No. 7

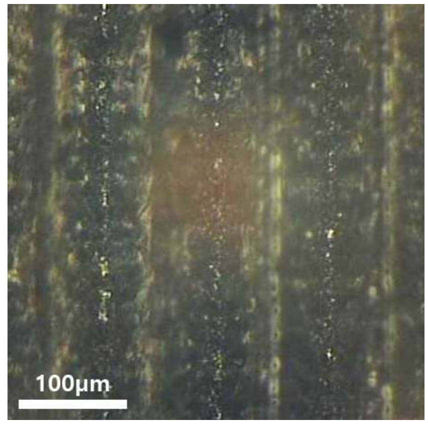


(h) No. 8

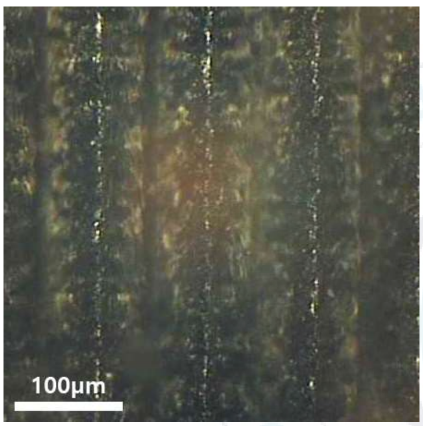


(i) No. 9

Fig. 4.6 Valleys of machined micro prism pattern (x600)

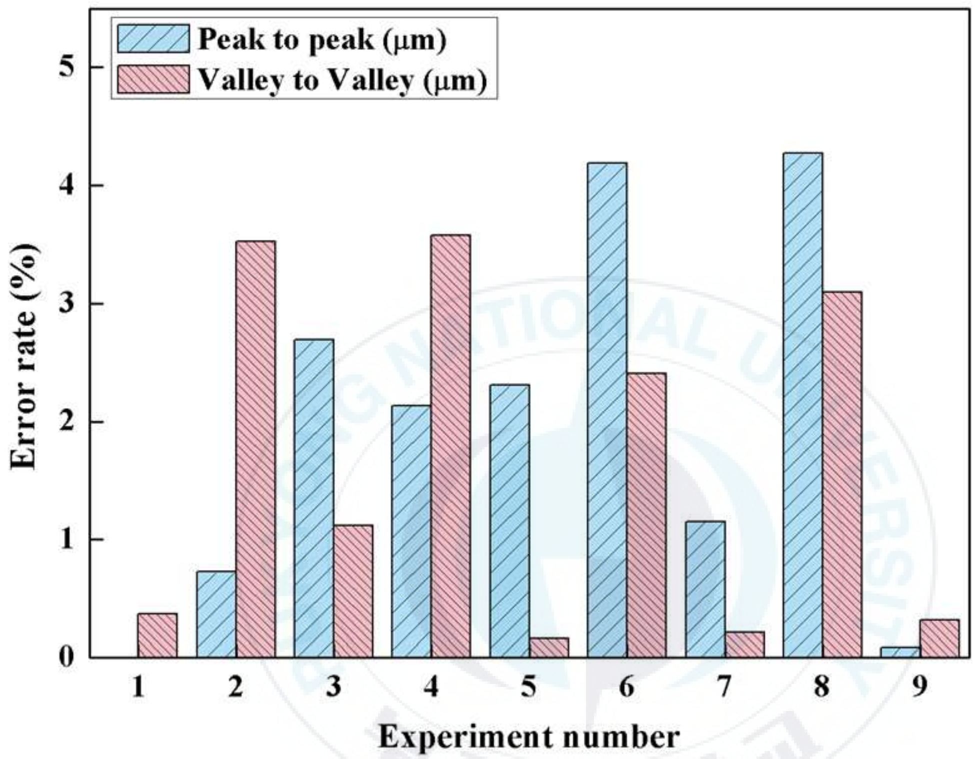


Fig. 4.7 Error rate on dimensional accuracy of micro prism pattern

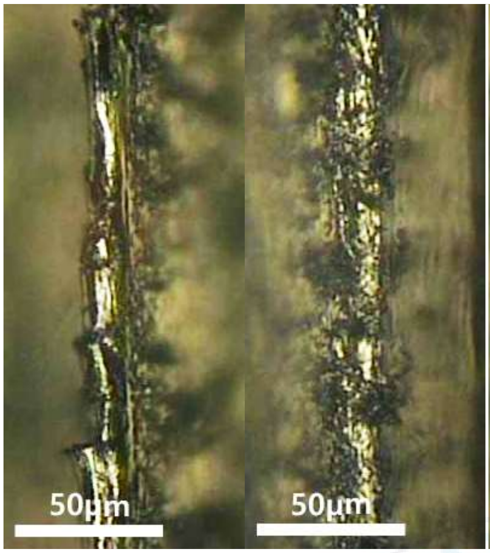

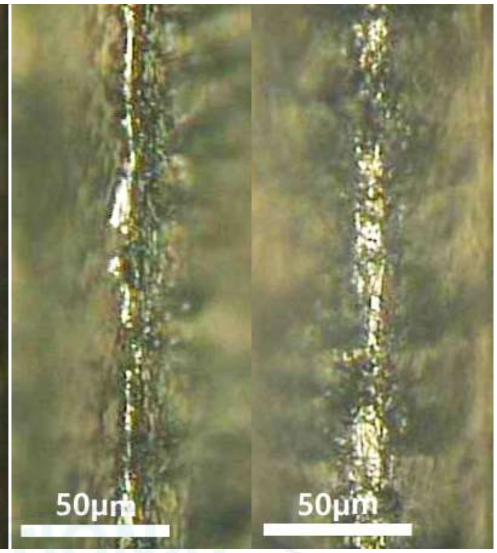


(a) No. 1 (b) No. 2

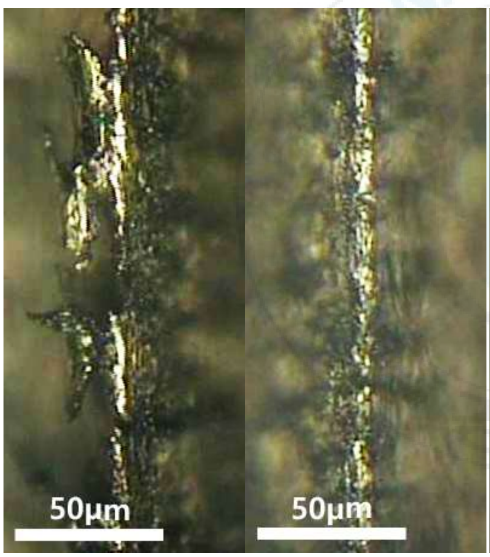

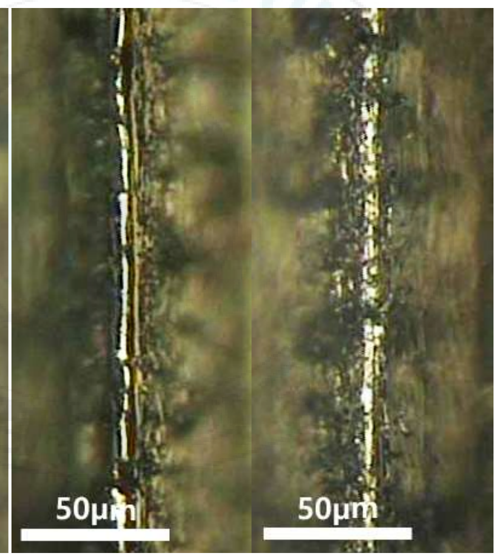


(c) No. 3 (d) No. 4

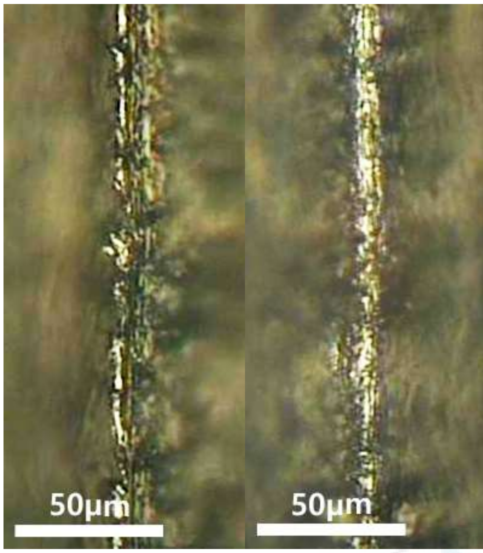


(e) No. 5

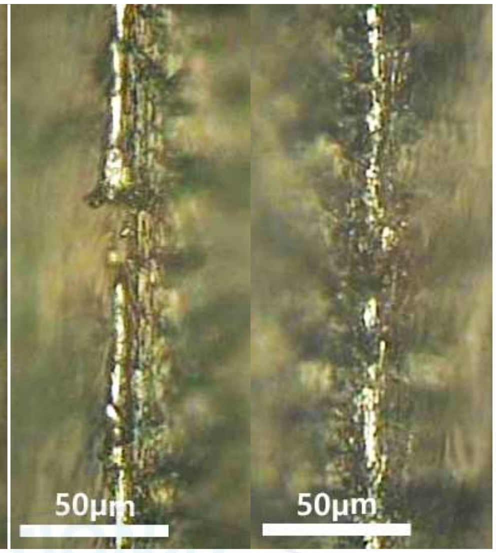


(f) No. 6

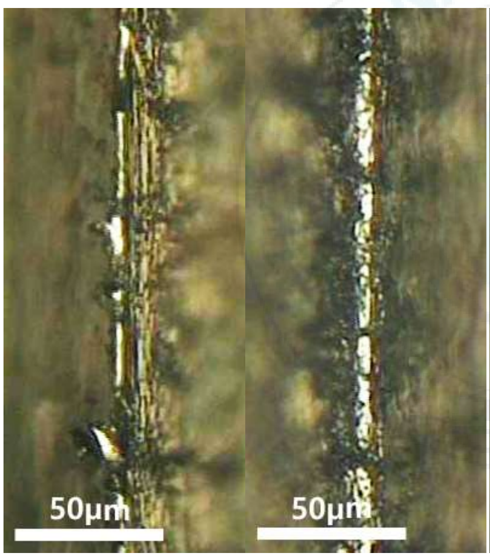


(g) No. 7

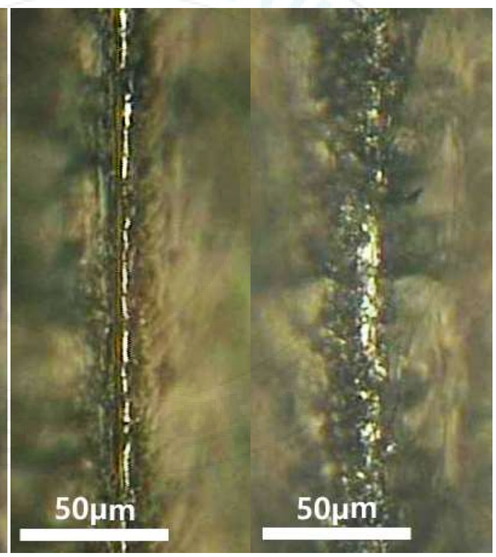


(h) No. 8

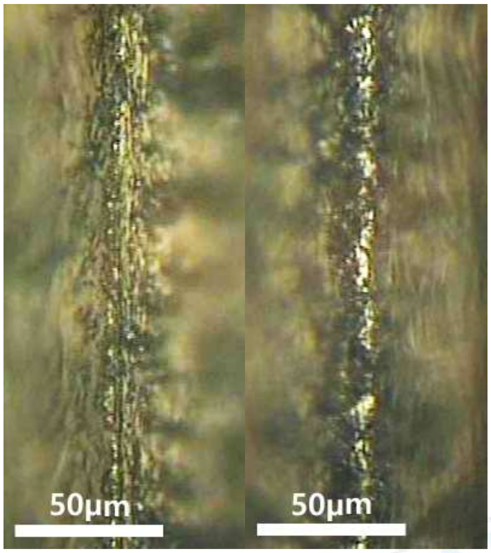


(i) No. 9

Fig. 4.8 Peak and valley of machined micro prism pattern (x1200)

## 4.3 Relation of tool wear and pattern accuracy

In this investigation, both wear of micro tool and pattern accuracy were measured and evaluated. To establish the effect of tool wear on accuracy of pattern, the relation of tool wear and peak to peak error was evaluated. Table 4.2 represents the correlation between SN ratio on tool wear and peak to peak error. Spearman's rank correlation coefficient is -0.3, which means the weak negative relation between two groups. It is considered because of larger deflection in micro prismatic end-milling. As Fig. 4.9 indicates, cutting force is applied in two opposite ways on end mill in traditional end-milling system. However in micro prismatic end-milling, cutting force acts only one direction, which makes larger deflection at micro end mill, especially bottom of the tool. It leads not only machining error but also decreasing of relation of tool wear and accuracy. The effect of deflection of tool is able to figure out in 3D model of machined micro prism pattern. Fig. 4.10 represents 3D model of the result of experiment No. 3 having largest tool wear, and Fig. 4.11 shows the one of experiment No. 7 having smallest tool wear. In experiment No. 3, the pattern height was 82.88μm, and 79.03μm in No. 7. This result also shows the negative relation with tool wear and machining error owing to deflection of tool.

Table 4.2 Correlation of tool wear and error on peak

| No. | SN ratio on wear | Error rate on peak (%) |
|---|---|---|
| 1 | -21.23 | 0.00 |
| 2 | -23.02 | 0.73 |
| 3 | -26.35 | 2.69 |
| 4 | -19.70 | 2.14 |
| 5 | -21.60 | 2.31 |
| 6 | -23.44 | 4.19 |
| 7 | -19.22 | 1.15 |
| 8 | -21.29 | 4.27 |
| 9 | -22.06 | 0.09 |

$\rho = -0.3$

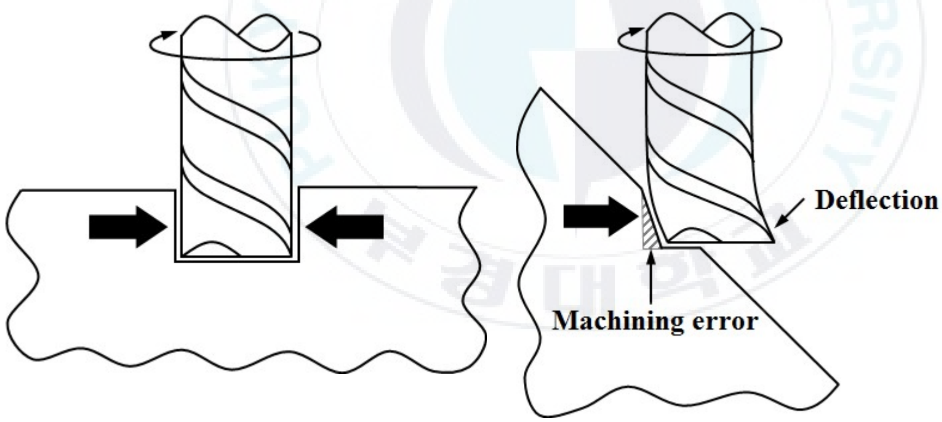


(a) Traditional end-milling (b) Micro prismatic end-milling

Fig. 4.9 Comparison of cutting force in traditional end-milling and micro prismatic end-milling

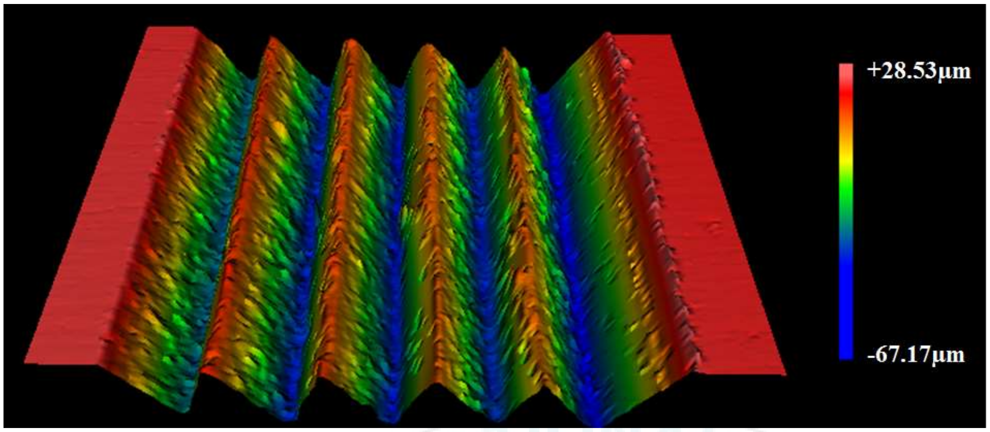


Fig. 4.10 3D model of experiment No. 3

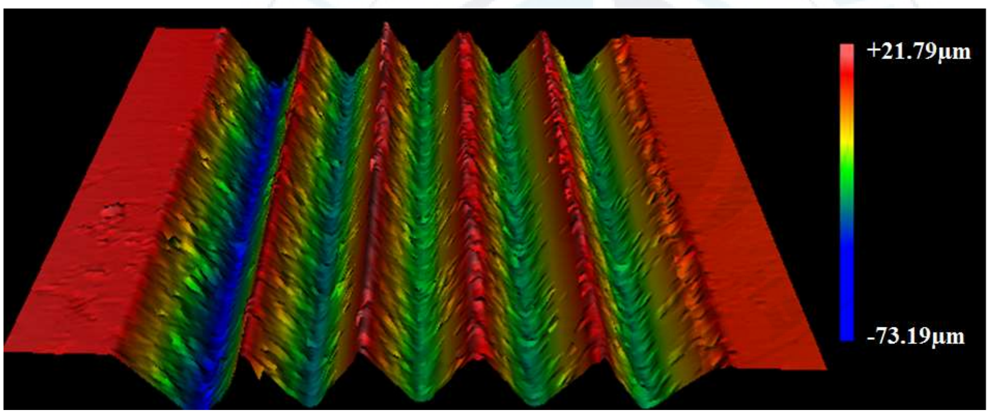


Fig. 4.11 3D model of experiment No. 7

# 5. Conclusions

In this paper, a micro prism pattern was fabricated by micro prismatic end-milling, and both flank wear and boundary wear of end mill were measured after machining. The effect of machining factors on tool wear was analyzed by design of experiment and ANOVA, and the conditions to minimize the wear were determined with experimental design. Analysis on dimensional accuracy and quality of micro prism pattern was also conducted. Thus following results are derived.

1. Micro prismatic end-milling was suggested and successfully conducted to fabricate the prism pattern having 100μm of pitch and height, 90° of angle.

2. After machining, flank wear and boundary wear were measured and evaluated to derive the condition to get minimum wear, 20,000rpm of spindle speed and 20mm/min of feed rate.

3. It is determined that the tool wear is proportional to the increase of spindle speed and the decrease of feed rate based on Taguchi method, and feed rate is statistically significant on the tool wear.

4. The best quality of micro prism pattern was fabricated when spindle speed is 20,000rpm and feed rate is 40mm/min.

# 감사의 글

벌써 2년 동안의 석사과정을 마무리 할 시간이 다가왔습니다. 새로운 경험, 그리고 많은 배움과 함께한 시간이었습니다. 졸업을 앞두고 감사의 말을 전하고 싶은 분들이 많아 감사의 글을 통해 조금이나마 전하고자 합니다. 먼저 바쁘신 가운데도 저의 석사과정과 학위논문을 무사히 마무리 할 수 있도록 성심성의껏 지도해주신 저의 지도교수님인 곽재섭 교수님께 깊은 감사를 드립니다. 그리고 귀중한 시간 내주셔서 학위논문을 세심히 심사해주시고 논문에 관해 많은 충고 해주신 강대민 교수님, 김태완 교수님께 감사드립니다.

초정밀지능가공 연구실의 선후배님들이 있어 무사히 논문을 마무리 할 수 있었습니다. 많은 조언해주신 이성호 교수님, 유만희 처장님, 방연일 선생님, 김주권 위원님, 곽태경 선생님 그리고 논문 작성에 많은 도움 주신 이희철 선배님 감사합니다. 학부생 때부터 많은 조언과 도움 주신 상오선배님, 창민선배, 태희선배, 한성선배, 창근선배, 병훈선배, 동현선배에게도 감사의 말을 전합니다. 2년 동안 함께 고생한 경아와 지은이에게도 감사와 축하를 전합니다. 아직 학위과정중인 다솜이와 언제나 열심히 공부하는 세영이와 수진이에게도 고맙다는 말을 전합니다.

마지막으로 항상 뒤에서 저를 응원해주는 부모님께 사랑과 감사를 전합니다. 두 분의 지지가 있었기에 여기까지 올 수 있었습니다. 다시 한 번 도와주신 많은 분들에게 감사드리며 이만 글을 마치겠습니다.

# REFERENCES


1. D. Ebert, B. Bhushan (2012) “Durable Lotus-effect surfaces with hierarchical structure using micro- and nanosized hydrophobic silica particles”, Journal of Colloid and Interface Science, Vol. 368, pp. 584~591

2. B. S. Kim, S. Shin, S. J. Shin, K. M. Kim, H. H. Cho (2011) “Micro-nano hybrid structures with manipulated wettability using a two-step silicon etching on a large area”, Nanoscale research letters, Vol. 6, No. 1, pp. 1~10

3. A. Funamoto, S. Aoyama (2006) “LED backlight system with double‾prism pattern”, Journal of the Society for Information Display, Vol. 14, No. 11, pp. 1045~1051

4. L. M. Griep, F. Wolbers, B. de Wagenaar, P. M. ter Braak, B. B. Weksler, I. A. Romero, P. O. Couraud, I. Vermes, A. D. van der Meer, A. van den Berg (2013) “BBB on chip: microfluidic platform to mechanically and biochemically modulate blood-brain barrier function”, Biomedical microdevices, Vol. 15, Issue 1, pp. 145~150

5. P. Guo, Y. Lu, P. Pei, K. F. Ehmann (2014) “Fast generation of micro-channels on cylindrical surfaces by elliptical vibration texturing”,

Journal of Manufacturing Science and Engineering, Vol. 136, No. 4, pp. 041008

6. B. C. Shin, S. J. Ha, M. H. Kang, Y. M. Heo, G. S. Yoon, M. W. Cho (2006) “The cutting process monitoring of micro machine using multi sensor”, Transactions of Materials Processing, Vol. 18, No. 2, pp. 144~149

7. E. Gentili, L. Tabaglio, F. Aggogeri (2005) “Review on micromachining techniques”, AMST’05 Advanced Manufacturing Systems and Technology, Vol. 486, pp. 387~396

8. J. W. Lee, S. J. Ha, K. P. Hong, Y. K. Cho, K. B. Kim, B. C. Kim, M. W. Cho (2016) “A study on the analysis method of shape quality and the micro burr removal on a micro pyramid pattern using the micro MR fluid jet polishing system”, Smart Materials and Structures, Vol. 25, No. 4, pp. 045001

9. Y. Deng, P. Yi, L. Peng, X. Lai, Z. Lin (2014) “Experimental investigation on the large-area fabrication of micro-pyramid arrays by roll-to-roll hot embossing on PVC film”, Journal of Micromechanics and Microengineering, Vol. 24, No. 4, pp. 045023

10. C. H. Bae, K. C. Heo, C. G. Jhun, B. J. Rvu, K. W. Koo (2015) “Design and fabrication of pattern structures of the light guide plate for enhanced brightness of backlight unit”, The Transactions of The Korean Institute of Electrical Engineers, Vol. 64, No. 2, pp. 310~314

11. C. H. Chien, Z. P. Chen (2009) “The study of integrated LED-backlight plate fabricated by micromachining technique”, Microsystem Technologies, Vol. 15, No. 3, pp. 383~389

12. M. K. Kwak, J. G. Ok, S. H. Lee, L. J. Guo (2015) “Visually tolerable tiling (VTT) for making a large-area flexible patterned surface”, Materials Horizons, Vol. 2, No. 1, pp. 86~90

13. Q. L. Deng, C. Y. Chen, S. W. Cheng, W. S. Sun, B. S. Lin (2012) “Micro-prism type single-lens 3D aircraft telescope system”, Optics Communications, Vol. 285, Issue 24, pp. 5001~5007

14. A. Funamoto, S. Aoyama (2006) “LED backlight system with double‾prism pattern”, Journal of the Society for Information Display, Vol. 14, No. 11, pp. 1045~1051

15. E. S. Park, T. J. Je, H. J. Choi, E. C. Jeon, M. C. Kang (2012) “Wear characteristics of V shape diamond tool for micro prism pattern with Al alloys”, Transactions of Nonferrous Metals Society of China, Vol. 22, pp.

s769~s774

16. Y. E. Yoo, T. H. Kim, T. J. Je, D. S. Choi, C. W. Kim, S. K. Kim (2011) “Injection molding of micro patterned PMMA plate”, Transactions of Nonferrous Metals Society of China, Vol. 21, pp. s148~s152

17. J. Kimmel (2012) “Review paper: diffractive backlight technologies for mobile applications”, Journal of the Society for Information Display, Vol. 20, No. 5, pp. 245~258

18. Y. Neuvo (2004) “Cellular phones as embedded systems”, In Solid-State Circuits Conference Digest of Technical Papers, pp. 32~37

19. A. Iranli, W. Lee, M. Pedram (2006) “HVS-aware dynamic backlight scaling in TFT-LCDs”, IEEE Transactions on Very Large Scale Integration (VLSI) Systems, Vol. 14, No. 10, pp. 1103~1116

20. A. Tagaya, M. Nagai, Y. Koike, K. Yokoyama (2001) “Thin liquid-crystal display backlight system with highly scattering optical transmission polymers”, Applied Optics, Vol. 40, No. 34, pp. 6274~6280

21. J. Hüttner, G. Kuhn, M. Winter (2008) “LED backlighting of LCDs in mobile appliances”, Mobile Displays: Technology and Applications, pp.

227~249

22. K. Kitamura (2007) “Wear of tool”, Transactions of Materials Processing, Vol. 16, No. 7, pp. 493~501

23. J. Jeong, H. Kwon, J. Koo, P. Kim, J. Kim (2012) “A study on machinability evaluation of Inconel 718 in flat end milling” Journal of the Korean Society of Manufacturing Technology Engineers, Vol. 21, No. 6, pp. 982~987

24. G. Taguchi (1977) “Experimental designs”, Tokyo: Maruzen Publishing Company

25. E. C. Jeon, T. J. Je, E. S. Lee, E. S. Park, J. R. Lee, H. Choi, S. Chang, S. K. Choi (2013) “Optimization of hybrid LED package system for energy saving based on micro machining technology and taguchi method”, International Journal of Precision Engineering and Manufacturing, Vol. 14, No. 6, pp. 1113~1116